Environ. Chem. **2016**, *13*, 50-57
doi:10.1071/EN14216_AC

Supplementary material

Physical long-term regeneration dynamics of soil organic matter as followed by ^{1}H solid-state NMR methods

Alexander Jäger,[A] *Jette Schwarz,*[B] *Yamuna Kunhi Mouvenchery,*[B] *Gabriele E. Schaumann*[B] *and Marko Bertmer*[A,C]

[A]Leipzig University, Institute for Experimental Physics II, Faculty for Physics and Earth Sciences, Linnéstraße 5, D-04109 Leipzig, Germany.

[B]University of Koblenz-Landau, Institute for Environmental Sciences, Group of Environmental and Soil Chemistry, Fortstraße 7, D-76829 Landau, Germany.

[C]Corresponding author. Email: bertmer@physik.uni-leipzig.de

Environ. Chem. **2016**, *13*, 50 ©CSIRO 2016
doi:10.1071/EN14216_AC

Proton mobility in SP depending on different water contents

The complete time series of SP7, SP12, SP18 and SP38 are shown in Fig. S1. It can be seen that the tendency to return to the initial mobility depends on the water content.

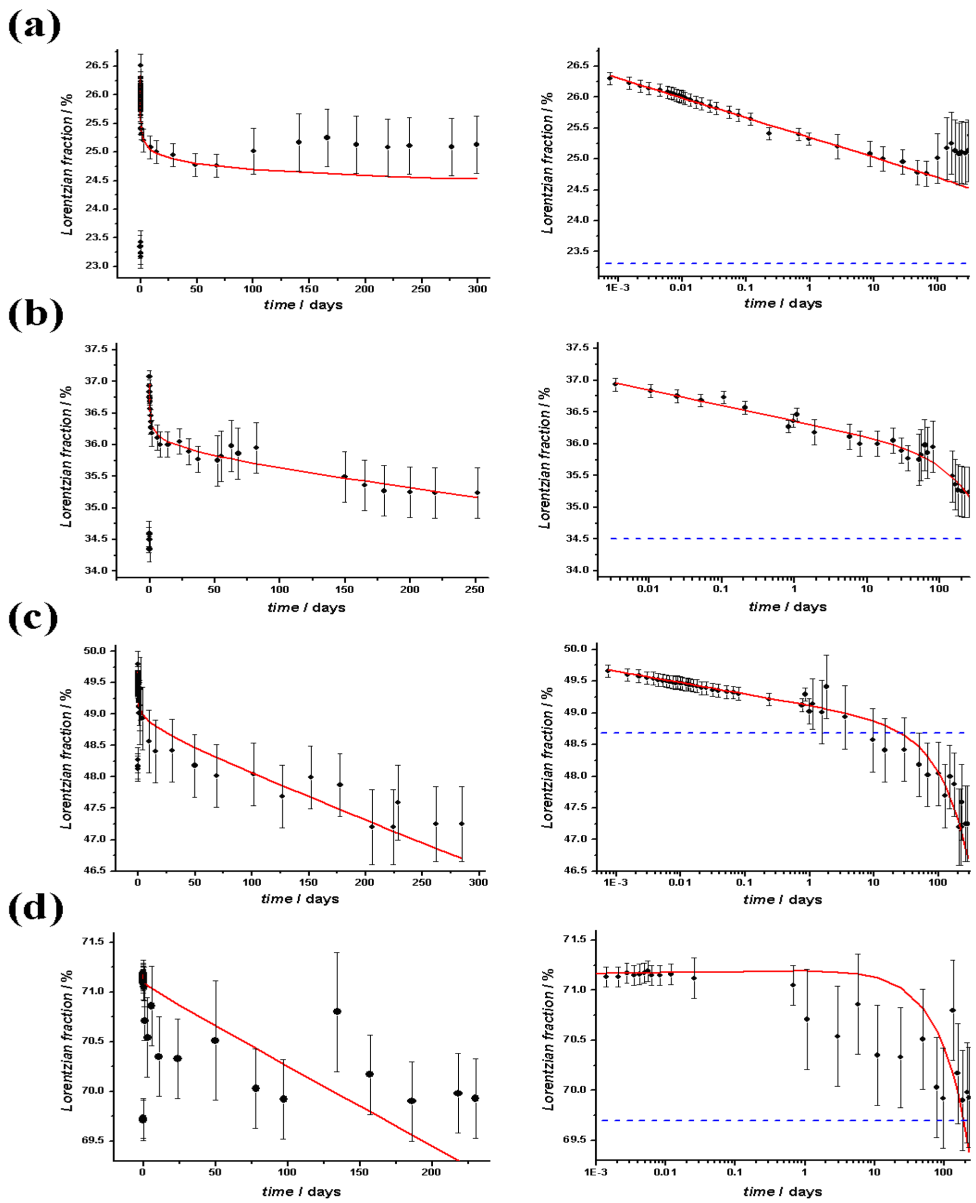

Fig. S1. Lorentzian fraction as a function of time for SP7 (a), SP12 (b), SP18 (c), and SP 38 (d) on a linear time scale (left) and on a logarithmic time scale (right).

The time series of sample SP38 (Fig. S1d) can only be fitted with large deviations to the model function Eqn 1. Particularly at the time point of the cut-off, we observed large uncertainties, which are difficult to explain at the moment. In the dessicator used for sample equilibration of SP38, we observed a kind of aggregation of the soil material that may be due to a kind of swelling effect. We can only assume that high water contents may also have a specific effect on physical aging. Nevertheless, the general trend is still recognisable.

Initial slow-down of proton mobility (100 min) depending on water content

For better comparison, in Fig. S2, the change of proton mobility for SP7, SP18 and SP38 is shown for the first 100 min after the heating event. They are displayed on a logarithmic time scale with the size of the symbols representing the size of the uncertainty. As can be seen, the slope of the data points (illustrating the decrease of mobility, logarithmic coefficient *A*) becomes more negative with decreasing water content.

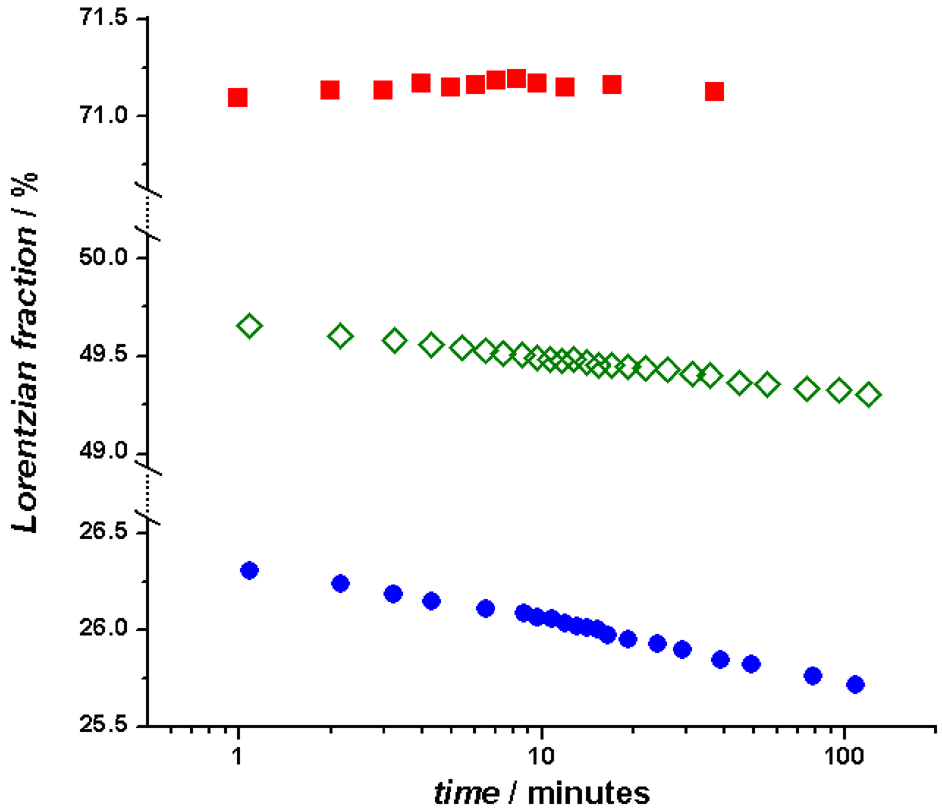

Fig. S2. Short-time behaviour on a logarithmic time scale for SP samples with different water content; SP38, squares, SP18, open diamonds; SP7, dots.

Reproducibility of the mobility increase

The anomalous mobility increase was tested at three different times of the year for air-dried SP. The results are shown in Fig. S3. Owing to the different ambient conditions (especially humidity), the initial Lorentzian fraction varies slightly.

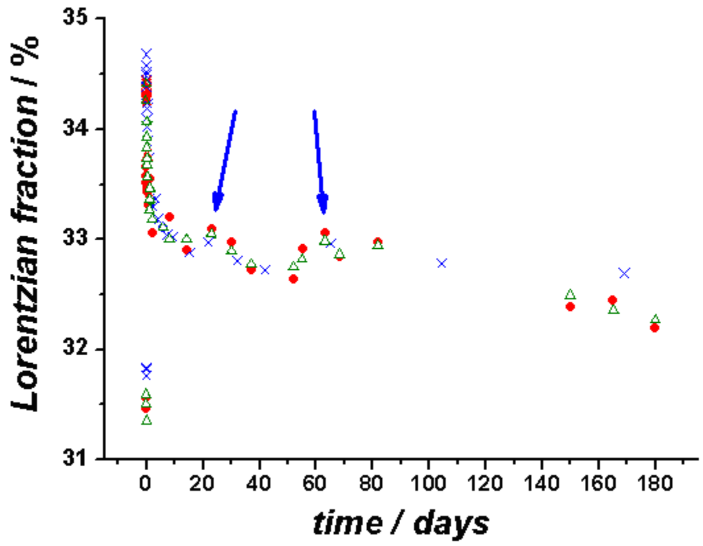

Fig. S3. Mobility increase (arrows) of three independent runs of air-dried SP. Because the basic mobile fraction varies slightly for each sample, the graphs were simply plotted on top of each other. It can be clearly seen that the mobility increase always happens at the same time.

Alternative fitting formula tested on basis of first-order reaction kinetics

The observed time series can in principle be fitted on the basis of several first-order reaction kinetics processes. At least three exponential components are required to obtain sufficient fit (Fig. S4) of the data. On the logarithmic scale, the difference with the Arrhenius approach becomes obvious for the first 24 h. Additionally, the linear term and the time-independent mobility have to be added, as summarised in Eqn S1. Because eight parameters must therefore be introduced, we decided not to use this type of fitting. This is especially true because one does not know from the beginning how many terms the equation has to have, i.e. how many different kinetic actors are present in the system.

$$y = A \cdot e^{(-t/B)} + C \cdot e^{(-t/D)} + E \cdot e^{(-t/F)} + G \cdot t + y_0 \quad \text{(S1)}$$

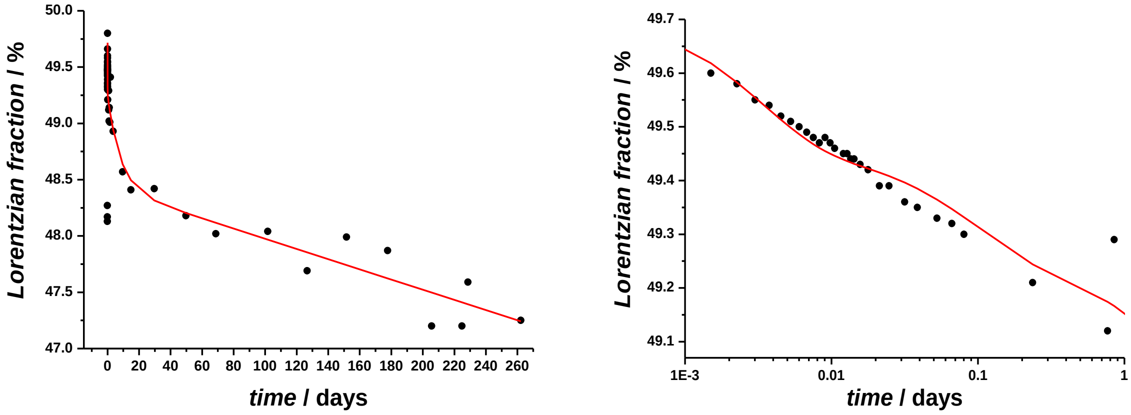

Fig. S4. Lorentzian fraction as a function of time for SP18 on a linear time scale (left) and on a logarithmic time scale (right) fitted with a multiexponential fit (Eqn S1).